Fibers and Polymers 2010, Vol.11, No.1, 1-7 DOI 10.1007/s12221-010-0001-4

Poly(ethylene 2,6-naphthalate)/MWNT Nanocomposites Prepared by In Situ Polymerization: Rheological and Mechanical Properties

Min Ho Jee, Jin Soo Lee, Ju Yong Lee, Young Gyu Jeong[1], and Doo Hyun Baik*

Department of Advanced Organic Materials and Textile System Engineering, Chungnam National University, Daejeon 305-764, Korea

[1]*School of Advanced Materials and System Engineering, Kumoh National Institute of Technology, Gumi 730-701, Korea*

(Received November 6, 2009; Revised November 26, 2009; Accepted December 11, 2009)

Abstract: Poly(ethylene 2,6-naphthalate)/multi-walled carbon nanotube (PEN/MWNT) nanocomposites are prepared by *in situ* condensation polymerization in the presence of various acid-treated MWNT (a-MWNT) contents and their morphology, rheological and mechanical properties are investigated as a function of the a-MWNT content. SEM image of a plasma-etched nanocomposite exhibits that a-MWNTs are dispersed well in the PEN matrix by forming an interconnected network structure. Accordingly, rheological properties such as complex viscosities and shear moduli of PEN/a-MWNT nanocomposites at the terminal region of low frequency are much higher than those of pure PEN. Glass transition temperatures of nanocomposites also increase with the increment of the a-MWNT content, which stems from the reduced chain mobility due to the specific interaction between a-MWNTs and PEN matrix. Dynamic and tensile mechanical properties of nanocomposites are also higher than those of pure PEN and they increase with the increment of the a-MWNT content. The highly improved mechanical properties of PEN/a-MWNT nanocomposites are explained to originate from the interconnected network structure of a-MWNTs in PEN matrix as well as the strong interfacial adhesion between a-MWNTs and PEN matrix.

Keywords: Poly(ethylene 2,6-naphthalate), Nanocomposite, Carbon nanotube, *In situ* polymerization, Physical properties

Introduction

Polymer nanocomposites including carbon nanotubes (CNTs) have attracted great attention from industry and academia as a new class of composite materials [1-9]. Since CNTs with large surface area and high aspect ratio exhibit a unique combination of mechanical, electrical, and thermal properties, they are considered as ideal reinforcing nanomaterials to improve or enhance the properties of conventional polymers [10-13]. However, CNTs in the polymer matrix have strong tendency to form aggregates due to the van der Waals interaction between themselves, which eventually leads to deterioration in composite properties [14]. For achieving enhanced physical properties of polymer/CNT nanocomposites, the dispersion of CNTs in the polymer matrix as well as the strong interfacial adhesion between CNTs and polymer matrix are critical factors to be controlled [15-20].

There are three common processing methods to manufacture polymer/CNT nanocomposites with high performances [21]. Solution mixing may be the most common method for fabricating polymer nanocomposites because CNTs can be efficiently de-aggregated and dispersed in a relevant solvent by agitation or sonication before evaporating the solvent to form a composite film [22]. By this method, high CNT loading of up to 50 wt% and reasonably good dispersion can be attained. Melt compounding uses high temperature and high shear forces to disperse CNTs in a polymer matrix. It is most effective method from industrial perspective [23,24]. However, compared to the solution mixing, the melt compounding is generally less effective at dispersion of CNTs in the polymer matrix and also it is limited to lower concentrations due to the high viscosities of the composites at higher CNT loadings. Similar to the solution mixing, *in situ* polymerization method can improve the initial dispersion of CNTs in the liquid state of monomers and consequently in the polymer composites. In addition, it is a very convenient processing technique, which allows the preparation of composites with high CNT loading and very good miscibility with most polymer type.

Poly(ethylene 2,6-naphthalate) (PEN) as an engineering thermoplastic possesses a higher end property spectrum in particular with regards to mechanical performance, thermal resistance, and barrier properties [25]. To further enhance the physical properties and thus expand the applications, PEN-based nanocomposites including nanofillers such as clay, silica have been investigated extensively [26,27]. Kim *et al.* have recently prepared PEN-based nanocomposites including multi-walled carbon nanotubes (MWNT) via melt compounding and investigated their crystallization behavior, mechanical and rheological properties [28,29]. We have also prepared nanocomposites based on PEN and acid-treated MWNT (a-MWNT) via *in situ* condensation polymerization and investigated the effect of a-MWNT on non-isothermal crystallization kinetics of the nanocomposites [30,31]. As a result, it was found that the crystallization rates of the nanocomposite with very low a-MWNT content of 0.01 wt% were much faster than that of pure PEN by two times due to the efficient nucleation of a-MWNTs dispersed in the PEN matrix [31].

*Corresponding author: dhbaik@cnu.ac.kr

On continuing our effort to delve PEN/a-MWNT nanocomposites prepared by *in situ* condensation polymerization, in this study, we have investigated rheological and mechanical properties of the nanocomposites containing very low a-MWNT contents (0.01, 0.05, and 0.10 wt%) by using scanning electron microscope, rheometer, dynamic mechanical analyzer, and universal tensile machine. The rheological and mechanical properties of PEN/a-MWNT nanocomposites are analyzed by correlating with the morphological features.

Experimental

Materials

The pristine MWNT (diameter of 10~15 nm, length of 10~20 μm, and purity of ~95 wt%), which was manufactured by CVD process, was supplied from Hanwha Nanotech Co. (Republic of Korea). Dimethyl 2,6-naphthalene dicarboxylate (NDC) and ethylene glycol (EG) as monomers for the PEN synthesis were purchased from BP Co. and Samchun Chemical Co., respectively. Titanium butoxide was used as the catalyst for the condensation polymerization.

Preparation of PEN/a-MWNT Nanocomposites

The acid-treated MWNT (a-MWNT) was prepared as follows. The pristine MWNT was added in a mixed solution of sulfuric acid and nitric acid (3/1, v/v) and the solution was refluxed at 140 °C for 20 min and cooled to room temperature. The solution was diluted by adding excess deionized water and then vacuum-filtered through PTFE membranes with 0.45 mm pores. The filtrate was washed with an excess of distilled water until the pH reached 7. The filtrated solid of a-MWNT was dried for 24 h at 80 °C under high vacuum. The structural characteristics of a-MWNT were well described in the previous report [30].

PEN/a-MWNT nanocomposites were prepared by *in situ* condensation polymerization, which consists of two step reactions of ester-interchange and polycondensation. The first ester-interchange reaction between NDC and EG (1/1.8 by mole ratio) was carried out in a custom-designed reactor at 210 °C, until the distillation of by-product (methanol) was ceased. After the ester-interchange reaction, excess EG/a-NWNT mixture, which was prepared by sonicating with a horn-type sonicator (Sonic dismembrator Model 500, Fisher Scientific Inc.), were added into the reactor. For the polycondensation reaction, the reactor was then progressively heated up to 280 °C and evacuated to low pressure below 1 mmHg. Excess EG was collected as the by-product during the polycondensation reaction. Finally, the reaction product was cooled into a water bath and then dried in a vacuum oven at 100 °C for 24 h. The a-MWNT contents were controlled to be 0.01, 0.05, and 0.10 wt% in the final product. For comparison, a pure PEN sample was also prepared by the same procedure without introduction of a-MWNT.

For structural analyses and property measurements of PEN/a-MWNT nanocomposites, amorphous films with 0.2 mm thickness were prepared by heating at 295 °C, applying a pressure of 500 psi, quenching into ice water, and drying in vacuum at 25 °C.

Characterization of PEN/a-MWNT Nanocomposites

The molecular weights of PEN homopolymer and nanocomposites were evaluated by measuring the intrinsic viscosities in phenol/TCE (6/4, w/w) solutions at 30 °C. In cases of PEN/a-MWNT nanocomposites, all the composite samples were dissolved in excess phenol/1,1,2,2-tetrachloroethane and filtered through the PTFE membrane to remove a-MWNTs from the PEN solution. The dissolution and filtration process were repeated several times. The final PEN solids were dried in vacuum at 100 °C for 24 h and then used for their intrinsic viscosities.

Morphological features of PEN/a-MWNT nanocomposites were characterized by using a cold-type FE-SEM (S4800, HITACHI). To identify the dispersion state of a-MWNT in the PEN matrix, nanocomposite films were etched with the oxygen plasma at 40 W for 90 sec.

Rheological properties of the pure PEN and PEN/a-MWNT nanocomposites in the melt-state were measured on a rheometer (ARES, TA Instrument Inc.) at 295 °C under the parallel-plate geometry with the plate diameter of 25 mm and the plate gap setting of 1 mm. Oscillatory shear measurements were performed by applying time-dependent strain, $\gamma(t)=\gamma_0\sin(\omega t)$, and measuring resultant shear stress, $\sigma(t)=\gamma_0(G'\sin(\omega t)+G''\cos(\omega t))$, where, ω, G', and G'' are the oscillation frequency of the rheometer, storage modulus, and loss modulus, respectively. The frequency range was varied between 0.03 and 400 rad/sec.

Dynamic thermal mechanical properties of PEN/a-MWNT nanocomposites were measured with a dynamic mechanical analyzer (DMA 7e, Perkin-Elmer). The sample dimensions were controlled to be 12×12.5×1.5 mm. The measurements were carried out under helium atmosphere from 30 to 180 °C at a heating rate of 5 °C/min. A dynamic force of 1000 mN and a static force of 1100 mN were applied with a frequency of 1 Hz.

Tensile mechanical properties of nanocomposites were measured with a universal tensile machine (Instron model 4467) with 30 N load cell. Measurements were performed at a crosshead speed of 0.2 mm/min. Five measurements were carried out for each sample and the resulting mechanical data were averaged.

Results and Discussion

Morphology of PEN/a-MWNT Nanocomposites

As noted above, the main advantage of *in situ* polymerization method is to disperse nanofillers effectively in the monomeric liquids and consequently in the nanocomposite matrix.

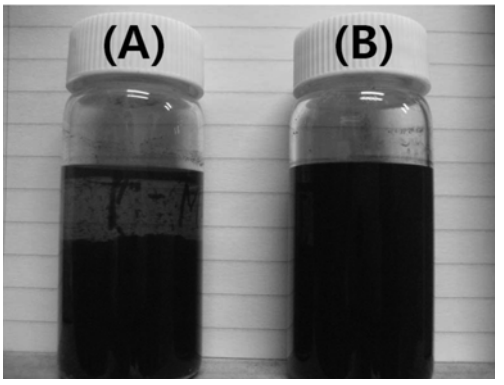

Figure 1. Optical photograph of pristine and acid-modified MWNT in ethylene glycol at 72 h after sonication; (A) pristine MWNT and (B) a-MWNT.

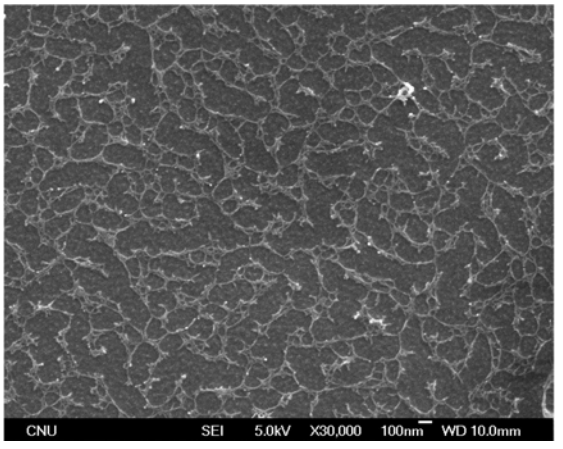

Figure 2. FE-SEM image of the oxygen plasma-etched PEN/a-MWNT nanocomposite film with 0.05 wt% a-MWNT content.

Figure 1 represents a optical photograph of pristine MWNT/EG and a-MWNT/EG solutions, which exhibit the dispersion state of pristine MWNT and a-MWNT in EG monomer. It was observed that the pristine MWNT was precipitated in EG (Figure 1(A)), whereas, a-MWNT was homogeneously dispersed in EG (Figure 1(B)). It suggests that, for a-MWNT/EG solution, there exists the specific interaction between carboxyl acid groups of a-MWNTs and hydroxyl groups of EG monomers.

Figure 2 shows a typical SEM image of oxygen plasma-etched PEN/a-MWNT nanocomposite with 0.05 wt% a-MWNT. Interestingly, a-MWNTs were found to be dispersed homogeneously in the PEN matrix by forming percolated network structure. This unique morphological feature is expected to significantly affect on the rheological and mechanical properties of PEN/a-MWNT nanocomposites, as will be discussed in the following section.

Rheological Properties of PEN/a-MWNT Nanocomposites

The frequency-dependent complex viscosities, $|\eta^*|$, of the pure PEN and PEN/a-MWNT nanocomposites with various a-MWNT contents are shown in Figure 3. At the terminal region of low frequency, the complex viscosities of samples increased with the increment of the a-MWNT content. Since the pure PEN and PEN/a-MWNT nanocomposites were synthesized independently, it is expected that rheological properties of PEN/a-MWNT nanocomposites in the melt state are strongly dependent on the a-MWNT content as well as the molecular weight of PEN matrix. For relative comparison of molecular weight among samples, intrinsic viscosities of pure PEN and PEN/a-MWNT nanocomposites were evaluated. As the result, the intrinsic viscosity of the pure PEN was measured to be 0.44 d*l*/g and the values of PEN matrix samples of nanocomposites were to be in the range of 0.43~0.46 d*l*/g. This result demonstrates that the effect of molecular weight on rheological properties of the pure PEN and PEN/a-MWNT nanocomposites is negligible. Compared with the pure PEN, the higher complex viscosities of nanocomposites are believed to originate from the good dispersion of a-MWNTs in the matrix as well as the strong interfacial adhesion between a-MWNTs and PEN matrix. In addition, it is expected that the higher complex viscosities of PEN/a-MWNT nanocomposites with higher a-MWNT content are owing to the strengthening of interconnected network structures of a-MWNTs in the PEN matrix.

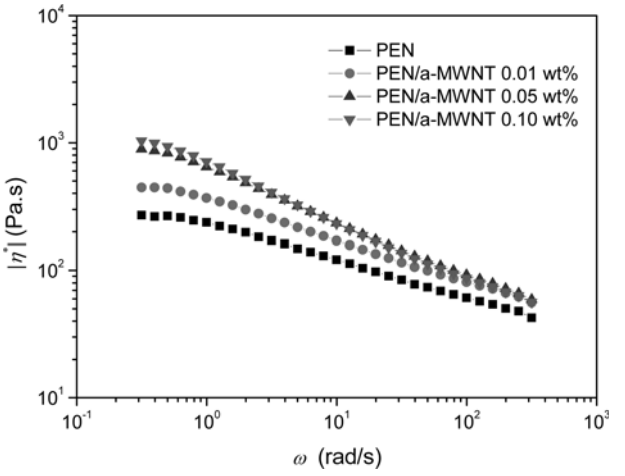

Figure 3. Complex viscosities of the pure PEN and PEN/a-MWNT nanocomposites as a function of frequency at 295 °C.

The complex viscosities of the pure PEN and PEN/a-MWNT nanocomposites decreased with increasing the frequency, which indicates the shear thinning as a typical non-newtonian behavior, as can be seen in Figure 3. In addition, at higher frequency, the complex viscosity difference between the pure PEN and nanocomposites became smaller. The stronger shear thinning behavior for the nanocomposite with higher a-MWNT content is associated with the orientation of a-MWNTs in the PEN matrix induced by the shear force developed at higher frequency. To identify the

influence of a-MWNT on the shear thinning of the pure PEN and PEN/a-MWNT nanocomposites, the shear thinning exponents (n) of all the samples were calculated by fitting a straight line to the data at low frequency based on the power law relationship of $|\eta^*| \approx \omega^n$. The resulting n values are found to decrease with increasing the a-MWNT content in the nanocomposites, as summarized in Table 1. This result indicates that the shear thinning behavior of PEN/a-MWNT nanocomposites become intense with increasing the a-MWNT content.

Table 1. Shear thinning exponents of complex viscosities ($|\eta^*|$), power law indices of shear storage and loss moduli (G' and G''), and glass transition temperatures (T_g) for pure PEN and PEN/a-MWNT nanocomposites

Materials	Shear thinning exponent	Power law index for G'	Power law index for G''	T_g (°C)
PEN	-0.11	1.30	0.84	118.3
PEN/MWNT 0.01 wt%	-0.17	1.13	0.76	120.9
PEN/MWNT 0.05 wt%	-0.28	0.97	0.61	122.0
PEN/MWNT 0.10 wt%	-0.32	0.88	0.54	124.0

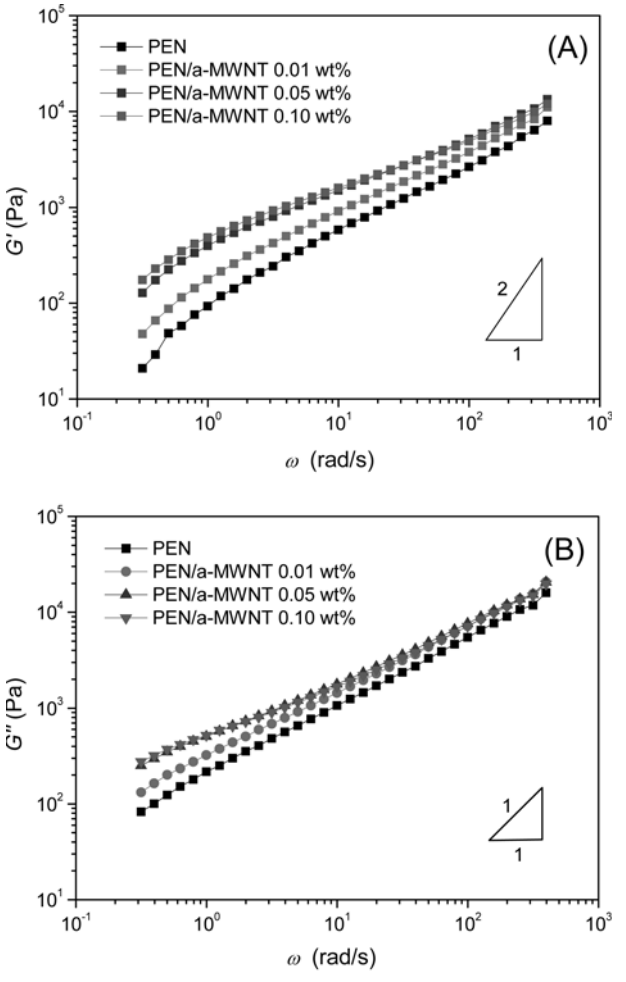

Figure 4. Shear storage moduli (A) and shear loss moduli (B) of pure PEN and PEN/a-MWNT nanocomposites as a function of frequency at 295 °C.

Shear storage modulus (G') and shear loss modulus (G'') of the pure PEN and PEN/a-MWNT nanocomposites as a function of frequency are shown in Figure 4. As the frequency and the a-MWNT content increased, both G' and G'' increased. It has been known that, if polymer chains are fully relaxed, they exhibit typical homopolymer-like terminal behavior at low frequency, which can be expressed by the power law relationship of $G' \approx \omega^2$ and $G'' \approx \omega^1$ for linear and monodisperse polymer melts. For the pure PEN, power law indices of $G'(\omega)$ and $G''(\omega)$ at low frequency were evaluated to be 1.30 and 0.84, respectively. These low power law indices of the pure PEN are probably due to the polydispersity of PEN chains. In cases of PEN/a-MWNT nanocomposites, frequency-dependent shear storage and loss modulus curves were fitted by the equations of $G' \approx \omega^{1.13\sim0.88}$ and $G'' \approx \omega^{0.76\sim0.54}$, respectively. Power law indices of $G'(\omega)$ and $G''(\omega)$ for PEN/a-MWNT nanocomposites were lower than the values of the pure PEN and decreased with increasing a-MWNT content in the nanocomposites, as listed in Table 1. This result indicates that the large-scale polymer relaxations in the nanocomposites are significantly restrained due to the percolated network structures of a-MWNT dispersed in the matrix.

Dynamic Mechanical Properties of PEN/a-MWNT Nanocomposites

Dynamic storage modulus (E') and loss tangent (tan δ) of the pure PEN and PEN/a-MWNT nanocomposites were examined as a function of temperature, as shown in Figure 5. The dynamic storage moduli for all the samples were relatively constant at the glassy state, decreased steeply at the glass transition region, and increased again at the rubbery state due to the cold-crystallization of PEN (Figure 5(A)). It was found that the storage moduli of PEN/a-MWNT nanocomposites below glass transition temperatures were far higher than those of the pure PEN, and they also increased with the a-MWNT content. It is believed that the improved dynamic mechanical properties for nanocomposites below glass transition temperatures are induced by the percolated network structure a-MWNTs in the PEN matrix as well as the good interfacial interaction between a-MWNTs and PEN matrix, which eventually leads to the effective external stress transfer from PEN matrix to a-MWNTs.

In the loss tangent versus temperature plots in Figure 5(B), the pure PEN and PEN/a-MWNT nanocomposites exhibit two distinct peaks: the sharp peak at lower temperature is associated with the glass transition temperature (T_g) and the shoulder peak at higher temperatures is related with the cold-crystallization temperature (T_c). The T_g of the pure PEN was measured to be 118.32 °C. For PEN/a-MWNT nanocomposites,

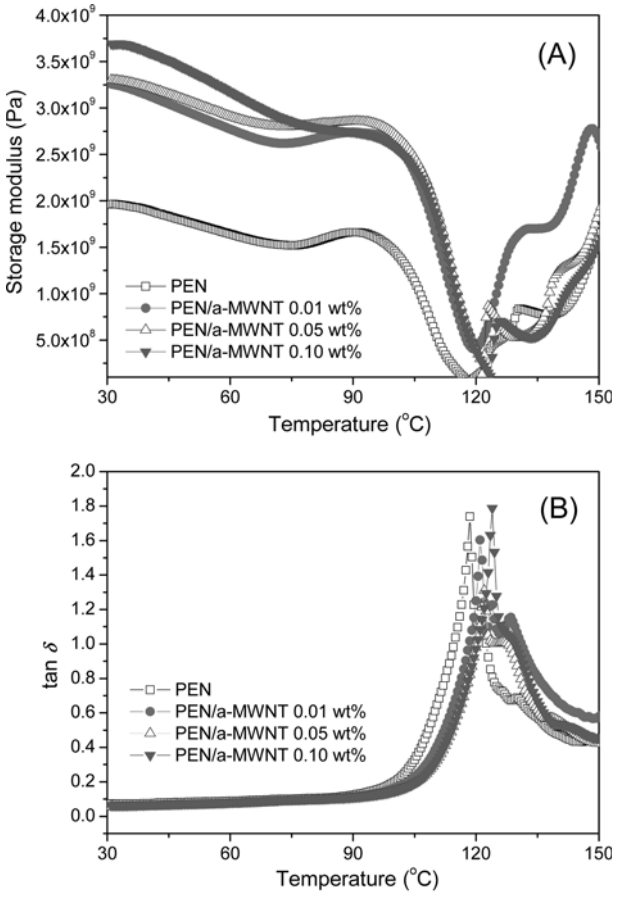

Figure 5. Storage moduli (A) and tan δ (B) of the pure PEN and PEN/a-MWNT nanocomposites as a function of temperature.

the T_g values were found to increase slightly with the increment of the a-MWNT content, as listed in Table 1. This result is caused by the restricted mobility of PEN chains due to the enhanced interfacial interactions between PEN matrix and a-MWNTs and the interconnected network structure of a-MWNTs in the matrix, which is intensified at higher a-MWNT content. Consequently, it is concluded that a-MWNTs incorporated into the PEN matrix reduce the chain mobility of the PEN matrix and thus lead to an increase in the dynamic storage modulus and glass transition temperature.

Tensile Mechanical Properties of PEN/a-MWNT Nanocomposites

Figure 6 displays typical tensile stress-strain curves of the pure PEN and PEN/a-MWNT nanocomposites with various a-MWNT contents at 30 °C. Tensile modulus and tensile strength of the pure PEN was measured to be 0.83 GPa and 46.1 MPa, respectively. In cases of PEN/a-MWNT nanocomposites, tensile mechanical properties were found to be significantly improved, compared to pure PEN, as summarized in Table 2. For instance, the tensile modulus and tensile strength of PEN/a-MWNT nanocomposite with 0.10 wt% a-MWNT were evaluated to be 1.05 GPa and 52.4 MPa, respectively. Similar to the dynamic mechanical properties, these improved tensile mechanical properties for PEN/a-MWNT nanocomposites were attributed to the strong interfacial interaction between a-MWNTs and PEN matrix as well as the good dispersion of a-MWNTs.

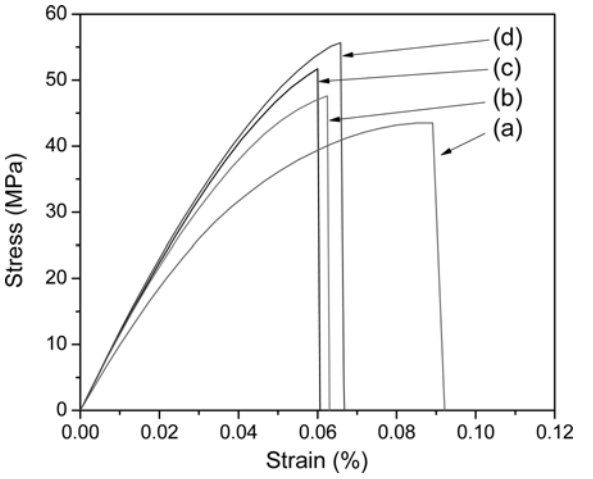

Figure 6. Stress-strain curves of (a) pure PEN, (b) PEN/a-MWNT 0.01 wt%, (c) PEN/a-MWNT 0.05 wt%, and (d) PEN/a-MWNT 0.10 wt%.

Table 2. Tensile modulus and strength of pure PEN and PEN/a-MWNT nanocomposites

Materials	Tensile modulus (GPa)	Tensile strength (MPa)
PEN	0.83±0.09	46.1±0.9
PEN/MWNT 0.01 wt%	0.97±0.12	48.4±4.6
PEN/MWNT 0.05 wt%	1.01±0.13	50.2±2.8
PEN/MWNT 0.10 wt%	1.05±0.09	52.4±3.1

Based on the assumption that a-MWNTs are randomly oriented in the PEN matrix and perfectly bonded with the matrix, the modulus, $E_{composite}$, of PEN/a-MWNT nanocomposites can be predicted by the following equation [21]

$$E_{composite} = \left[\left(\frac{3}{8}\right)\left(\frac{1+2\left(\frac{l_{MWNT}}{d_{MWNT}}\right)\eta_L V_{MWNT}}{1-\eta_L V_{MWNT}} \right) + \left(\frac{5}{8}\right)\left(\frac{1+2\eta_T V_{MWNT}}{1-\eta_T V_{MWNT}} \right) \right] E_{PEN} \quad (1)$$

$$\eta_L = \frac{\left(\frac{E_{MWNT}}{E_{PEN}}\right)-1}{\left(\frac{E_{MWNT}}{E_{PEN}}\right)+2\left(\frac{l_{MWNT}}{d_{MWNT}}\right)}$$

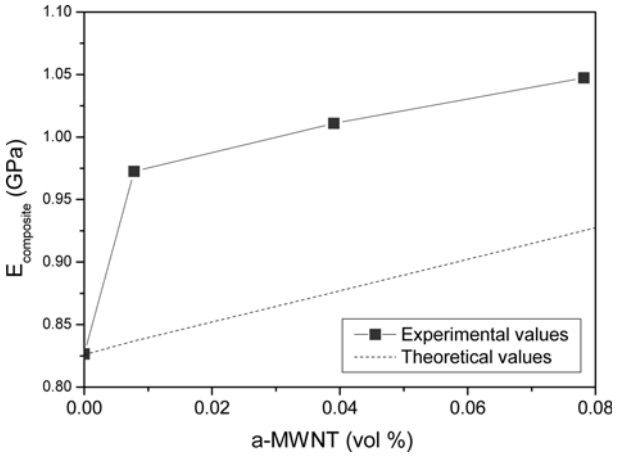

Figure 7. Comparison of experimental tensile moduli of PEN/a-MWNT nanocomposites with the theoretical values predicted from the equation (1).

$$\eta_T = \frac{\left(\frac{E_{MWNT}}{E_{PEN}}\right) - 1}{\left(\frac{E_{MWNT}}{E_{PEN}}\right) + 2}$$

where, E_{MWNT} and E_{PEN} are the tensile moduli of MWNT (~400 GPa) and pure PEN (~0.83 GPa), respectively. l_{MWNT}, d_{MWNT}, and V_{MWNT} are the length (~15 μm), diameter (~12.5 nm), and volume fraction of MWNT, respectively. V_{MWNT} can be easily calculated from the weight fraction of MWNT, MWNT density (1.8 g/cm^3), and amorphous PEN density (1.407 g/cm^3). Figure 7 shows the comparison of experimental tensile moduli of PEN/a-MWNT nanocomposites with the theoretical values predicted by the equation (1). Interestingly, it was found that the experimental tensile moduli were far higher than the theoretical values over the MWNT content investigated in this study. The unexpectedly high tensile moduli of PEN/a-MWNT nanocomposite are believed to arise from the good interfacial adhesion between a-MWNTs and PEN matrix as well as the dispersion state of a-MWNT with interconnected network structure.

Conclusion

In this study, rheological and mechanical properties of PEN/a-MWNT nanocomposites, which were prepared by *in situ* condensation polymerization, were investigated as a function of the a-MWNT content (0.01, 0.05 and 0.10 wt%). It was observed that, unlike pristine MWNTs, a-MWNTs were well dispersed in ethylene glycol without forming aggregates or precipitates, suggesting that a-MWNTs could interact strongly with PEM matrix. SEM image of plasma-etched PEN/a-MWNT nanocomposite also demonstrated that a-MWNTs were well dispersed in the PEN matrix by exhibiting a unique interconnected or percolated network structure. As the results, rheological and mechanical properties of PEN/a-MWNT nanocomposites were found to be strongly dependent on the a-MWNT content. The complex viscosities at the terminal zone of low frequency were significantly increased with increasing the a-MWNT content. The dynamic and tensile mechanical data also showed that storage moduli, T_g values, tensile moduli, and tensile strengths of nanocomposites increased with the increment of the a-MWNT content. For instance, the tensile modulus and strength of PEN/a-MWNT nanocomposite with a-MWNT content of 0.10 wt% were increased by 22 and 13 %, respectively, compared with the pure PEN. Overall, it was concluded that the highly improved dynamic and tensile mechanical properties of PEN/a-MWNT nanocomposites with very low a-MWNT content are achieved by the percolated network structure a-MWNTs in the PEN matrix as well as the good interfacial adhesion between a-MWNT and PEN matrix.

Acknowledgement

This study was supported by a grant from the Fundamental R&D Program for Core Technology of Materials funded by the Ministry of Knowledge Economy, Republic of Korea.

References

1. M. Wu and L. L. Shaw, *Inter. J. Hydrogen Energy*, **30**, 373 (2005).
2. R. Andrews and M. C. Weisenberger, *Cur. Opi. Sol. Sta. and Mater. Sci.*, **8**, 31 (2004).
3. P. Xue, K. H. Park, X. M. Tao, W. Chen, and X. Y. Cheng, *Compos. Struct.*, **78**, 271 (2007).
4. Z. Li, G. Luo, F. Wei, and Y. Huang, *Compos. Sci. Technol.*, **66**, 1022 (2006).
5. P. Liu, *Eur. Polym. J.*, **41**, 2693 (2005).
6. S. H. Jin, D. K. Choi, and D. S. Lee, *Coll. Sur. A*, **313**, 242 (2008).
7. K. Zhang, J. Y. Lim, and H. J. Choi, *Dia. & Rel. Mater.*, **18**, 316 (2009).
8. J. Y. Kim, D. K. Kim, and S. H. Kim, *Eur. Polym. J.*, **45**, 316 (2009).
9. A. C. Brosse, S. T. Girault, P. M. Piccione, and L. Leibler, *Polym.*, **49**, 4680 (2008).
10. C. A. Cooper, R. J. Young, and M. Halsall, *Compos. Part A*, **32**, 401 (2001).
11. P. L. Mceuen, M. Bockrath, D. H. Cobden, Y. G. Yoon, and S. G. Louie, *Phys. Rev. Lett.*, **83**, 5098 (1999).
12. G. Gao, T. Cagin, and W. A. Goddard, *Nanotechnology*, **9**, 184 (1998).
13. T. Uchida and S. Kumar, *J. Appl. Polym. Sci.,* **98**, 985 (2005).
14. B. Fiedler, F. H. Gojny, M. H. G. Wichmann, M. C. M. Nolte, and K. Schulte, *Compos. Sci. Technol.*, **66**, 3115 (2006).
15. M. Moniruzzaman and K. Winey, *Macromolecules*, **39**,

5194 (2006).
16. E. Camponeschi, R. Vance, M. Al-Haik, H. Garmestani, and R. Tannenbaum, *Carbon*, **45**, 2037 (2007).
17. U. A. Handge and P. Potschke, *Rheol. Acta*., **46**, 889 (2007).
18. J. T. Yoon, Y. G. Jeong, S. C. Lee, and B. G. Min, *Polym. Adv. Tech.*, **20**, 631 (2009).
19. J. Y. Kim, S. I. Han, and S. P. Hong, *Polymer*, **49**, 3335 (2008).
20. M. J. Green, N. Behabtu, M. Pasquali, and W. W. Adams, *Polymer*, **50**, 4979 (2009).
21. J. N. Coleman, U. Khan, W. J. Blau, and Y. K. Gun'ko, *Carbon*, **44**, 1624 (2006).
22. C. Bartholome, P. Miaudet, A. Derre, M. Maugey, O. Roubeau, C. Zakri, and P. Poulin, *Compos. Sci. Technol.*, **68**, 2568 (2008).
23. M. Wang, W. Wang, T. Liu, and W. D. Zhang, *Compos. Sci. Technol.*, **68**, 2498 (2008).
24. C. C. Teng, C. C. M. Ma, Y. W. Huang, S. M. Yuen, C. C. Weng, C. H. Chen, and S. F. Su, *Composites: Part A*, **39**, 1869 (2008).
25. A. E. Tonelli, *Polymer*, **43**, 637 (2002).
26. S. H. Kim, S. H. Ahn, and T. Hirai, *Polymer*, **44**, 5626 (2003).
27. T. M. Wu and C. Y. Liu, *Polymer*, **46**, 5621 (2005).
28. J. Y. Kim, H. S. Park, and S. H. Kim, *Polymer*, **47**, 1379 (2006).
29. J. Y. Kim and S. H. Kim, *J. Appl. Polym. Sci. Part B: Polym. Phys.*, **44**, 1062 (2006).
30. M. H. Jee, M. H. Lee, Y. H. Yoon, and D. H. Baik, *Text. Sci. Eng.*, **45**, 26 (2008).
31. M. H. Jee, M. H. Lee, Y. H. Yoon, and D. H. Baik, *Text. Sci. Eng.*, **45**, 33 (2008).